atmosphere

MDPI

Article

Effects of COVID-19 Control Measures on the Concentration and Composition of $PM_{2.5}$-Bound Polycyclic Aromatic Hydrocarbons in Shanghai

Jialiang Feng [1], Fan Fan [1], Yi Feng [1], Ming Hu [2], Jia Chen [2], Yutong Shen [3], Qingyan Fu [2] and Shunyao Wang [1,*]

1 School of Environmental and Chemical Engineering, Shanghai University, Shanghai 200444, China
2 Shanghai Environmental Monitoring Center, Shanghai 200235, China
3 Department of Communication, University of Ottawa, Ottawa, ON K1N 6N5, Canada
* Correspondence: syw@shu.edu.cn

Abstract: In order to explore the effects of COVID-19 control measures on the concentration and composition of $PM_{2.5}$-bound polycyclic aromatic hydrocarbons (PAHs), and to better understand the sources of $PM_{2.5}$-bound PAHs, $PM_{2.5}$, samples were collected at two sites in urban and suburban areas of Shanghai before the lockdown, during the lockdown, after the lockdown in 2020, and during the same periods in 2019. The mass concentrations of 21 individual PAHs were determined via GC-MS analysis. While the COVID-19 control measures significantly reduced the absolute concentration of $PM_{2.5}$-bound PAHs, they had no significant effect on their relative abundances, indicating that the significantly reduced traffic emission may not originally be the major source of PAHs in Shanghai. The differences in the composition of $PM_{2.5}$-bound PAHs at three different lockdown-related periods may be caused by the gas-particle distribution of semi-volatile PAHs. The similarity in the composition of $PM_{2.5}$-bound PAHs in different functional areas and different periods brings more uncertainties to the identification of PAH sources using the diagnostic ratios. During the lockdown period, the toxic equivalent concentration of $PM_{2.5}$-bound PAHs in Shanghai was estimated to decrease by about 1/4, which still exhibits substantial carcinogenic risk upon exposure via inhalation.

Keywords: $PM_{2.5}$; PAHs; COVID-19; lockdown measures; Shanghai

check for updates

Citation: Feng, J.; Fan, F.; Feng, Y.; Hu, M.; Chen, J.; Shen, Y.; Fu, Q.; Wang, S. Effects of COVID-19 Control Measures on the Concentration and Composition of $PM_{2.5}$-Bound Polycyclic Aromatic Hydrocarbons in Shanghai. *Atmosphere* **2023**, *14*, 95. https://doi.org/10.3390/atmos14010095

Academic Editor: Célia Alves

Received: 18 November 2022
Revised: 8 December 2022
Accepted: 20 December 2022
Published: 1 January 2023

1. Introduction

Polycyclic aromatic hydrocarbons (PAHs) are a class of highly toxic and harmful persistent organic pollutants in the atmosphere, with molecular structures containing two or multiple fused aromatic rings [1–3]. PAHs are released into the environment either from anthropogenic or natural sources. Anthropogenic sources refer to the formation of PAHs caused by incomplete combustion and pyrolysis of coal, petroleum, gasoline, and biomass [4–9]. The natural emission sources of PAHs mainly include volcanic eruption, forest fire, and diagenesis, etc. [10,11]. PAHs are identified as major toxic compounds with significant carcinogenicity and mutagenicity in an urban atmosphere [2,12,13]. Previous studies have shown that particulate PAHs in the atmosphere primarily exist in fine particulate matter ($PM_{2.5}$), for which industrial processes, automobile exhaust, power generation, waste incineration, biomass combustion, and coal combustion are the main sources of PAHs in urban areas [14–16]. In a previous study, the total of particulate PAHs in Beijing was found to be significantly higher (7.2 times) in the heating season (305.1 ± 279.0 ng m^{-3}, n = 33) compared to the non-heating season (42.3 ± 32.0 ng m^{-3}, n = 31) [17]. According to previous measurements, the abundance of individual PAHs can be several ng m^{-3} in $PM_{2.5}$ samples collected in Shanghai [18–20]. However, due to the similarity in the composition of PAHs generated from different combustion processes, there is still a lack of understanding of the sources of PAHs in $PM_{2.5}$ in an urban environment, which brings challenges to the regulation of PAH emission and public health.

In December 2019, a large number of pneumonia cases with unknown etiology were reported in Wuhan, followed by the outbreak of COVID-19 and lockdown measures in China [21–23]. Like other parts of the country, Shanghai launched the public health first-level emergency response on 24th January 2020, and implemented strict control policies. In order to control the pandemic, it was recommended to minimize unnecessary contact and maintain social distancing. Most public places were shut down, large-scale public activities were mostly canceled, industrial activities were reduced, and traffic activities were also stringently regulated to the minimum mode. Management and control measures have played a very positive role in controlling the epidemic situation, with significant improvement in urban air quality [24–26], which created a unique window for assessing the impact of anthropogenic activities on urban air pollution. The source and environmental fate of PAHs are both challenging topics in the field [27,28]. The present study considers the control measures of COVID-19 in 2020 as a large-scale air emission reduction experiment. Taking Shanghai, one of the megacities in China, as an example, the potential impacts of anthropogenic emission reduction on the absolute concentration and relative composition of PAHs in $PM_{2.5}$ under the control measures of COVID-19 were analyzed and discussed. We found the absolute abundance of PAHs decreased while their relative compositions remained at a similar level under the impact of the COVID-19 lockdown, indicating that traffic may not be a dominant and unique source of PAHs in Shanghai. Overall, our study shed light on the source identification of particulate PAHs in Shanghai, which further provides scientific insights for the mitigation of urban air quality in megacities.

2. Materials and Methods

2.1. Field Sampling

In order to understand the impact of the COVID-19 lockdown on $PM_{2.5}$ in different functional regions, we collected $PM_{2.5}$ samples from an urban (Pudong, PD) and suburban site (Dianshan lake of Qingpu, DS) in Shanghai (Figure 1). The PD sampling site (121.54° E, 31.23° N) is located in the center of Shanghai with a sampling height of 20 m, which is surrounded by residential and commercial areas. The DS sampling site (120.98° E, 31.09° N) is located near Dianshan Lake with a sampling height of 10 m. It is surrounded by a large area of vegetation and the lake and is only 1 km away from the G50 Shanghai-Chongqing highway, which is a typical suburban area. However, the DS site is also frequently influenced by emissions from surrounding industry, which can serve as a representative of an area with relatively poor air quality in Shanghai.

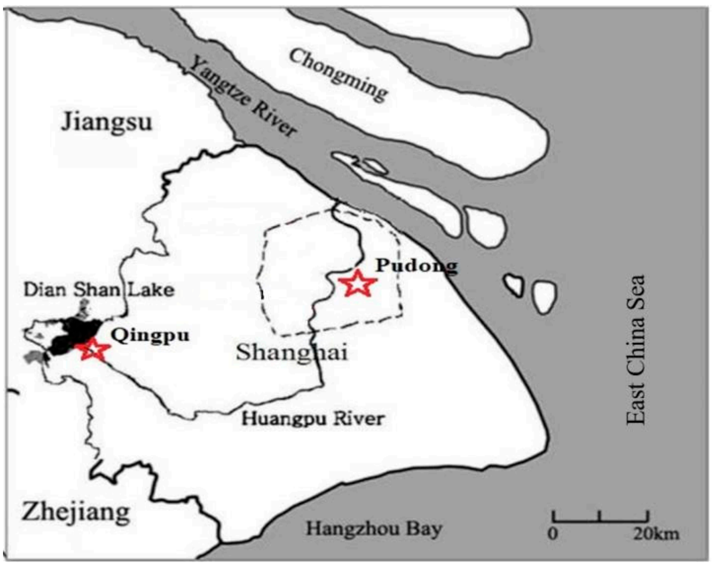

Figure 1. Location of sampling sites in Pudong New Area and Qingpu District of Shanghai (red star).

Samples were collected every 5 days from December 2018 to June 2019 and every 3 days from December 2019 to June 2020 using a high-volume $PM_{2.5}$ sampler (Thermo-Andersen, Franklin Massachusetts, USA) at both sites simultaneously. The sampling flow rate was controlled to be 1.13 $m^3\ min^{-1}$. Quartz filters (QM-A, 20.0 cm $\times$ 25.4 cm, Whatman, Buckinghamshire, UK) were used for $PM_{2.5}$ sampling, and a 4 h pre-baking at 450 °C was applied before sampling in order to remove all the volatile organic compounds (VOCs) on the blank filter. All sample collections started at 10:00 am on the first day and stopped at 10:00 am on the next day. In total, 215 $PM_{2.5}$ samples were collected. All filters were placed under a constant condition with 20 °C and 45% relative humidity for 24 h prior to mass weighing.

According to the pandemic lockdown timing, sampling duration was further categorized into before the lockdown period (BL, before the first level of action on 24 January 2020), during the lockdown period (DL, during the first level action), and after the lockdown period (AL, between March 24th when the first level action finished and 30 June 2020). For comparison, the corresponding periods in 2018–2019 were denoted as bL, dL, and aL, respectively.

2.2. Experimental Methods

The sample preparation and measurement procedure of PAH analysis can be referenced in our previous work [29]. Briefly, a specific area of the filter was punched and extracted 3 times by ultrasonication in dichloromethane at room temperature after being spiked with a mixture of deuterated PAH standards. Each extraction lasted for 30 min. Hexamethylbenzene was added to the extract as an internal standard prior to GC-MS (6890/5975, Agilent, Santa Clara, CA, USA) analysis under the selected ion mode. In the present study, 21 individual PAH compounds in $PM_{2.5}$ were identified and quantified, including phenanthrene (Phe), anthracene (Ant), retene (Ret), fluoranthene (Flu), acenaphthene (Ace), pyrene (Pyr), benzo[ghi]fluoranthene (BghiF), cyclopenta[cd]pyrene (CcdP), benz[a]anthracene (BaA), chrysene (Chr), m-tetraphenyl (m-QP), benzo[b+k]fluoranthene (BbkF), benzo[a]fluoranthene (BaF), benzo[e]pyrene (BeP), benzo[a]pyrene (BaP), perylene (Per), dibenzo[ah]anthracene (DBahA), anthanthracene (Anth), indeno [1,2,3-cd]pyrene (IcdP), benzo[ghi]perylene (BghiP), and coronene (Cor).

The QA/QC during the measurement of PAHs were carefully handled. Field blanks, filter blanks and solvent blanks were determined. No target compound was found in the blank samples. Relative response factors for standard compounds including PAHs to the internal standard were calculated. The mean recovery efficiency for all $PM_{2.5}$ samples was 61% $\pm$ 12% for Nap-d8, 71% $\pm$ 10% for Ace-d10, 78% $\pm$ 13% for Phe-d10, 85% $\pm$ 15% for Chr-d12, and 84% $\pm$ 12% for Per-d12, respectively.

2.3. Potential Toxicity of PAHs

The toxic equivalency factor (TEF) can be used to estimate the toxicities of PAHs in $PM_{2.5}$ samples [30–32]. Among all types of PAHs, BaP was recognized as a reference compound due to its high carcinogenic potential, and the carcinogenicity of a specific PAH is calculated relative to BaP [33–35]. By adopting the method recommended by the World Health Organization (WHO), the benzo[a]pyrene equivalent (BaP_{eq}) of each specific PAH can be calculated using Equation (1).

$$BaP_{eq} = \sum C_i \times TEF_i \tag{1}$$

where C_i is the concentration of a specific PAH (ng m^{-3}) and TEF_i stands for toxic equivalency factor. In the current work, the TEF_i was set as 0.001 for Phe, Flu, Ace, Pyr, Ret, BghiF, CcdP, BaF, Per, Anth, Cor, and QP; 0.01 for Ant, Chr, BeP, and BghiP; 0.1 for BaA, BbkF, and IcdP; 1 for BaP and DBahA, respectively.

Based on the estimated BaP_{eq}, the incremental lifetime cancer risk (ILCR) can be calculated using the following equation:

$$ILCR = BaP_{eq} \times UR_{BaP} \quad (2)$$

where UR_{BaP} is the unit cancer risk $(ng\ m^{-3})^{-1}$. The WHO recommended the ILCR value is 8.7×10^{-5}, representing an occurrence of 87 more cancer patients in 1 million people when the BaP exposure level increased by 1 ng m^{-3} within a normal whole lifetime (70 years). It has been defined as low cancer risk for ILCR < 10^{-6}, potentially medium cancer risk for 10^{-6} < ILCR < 10^{-4}, and relatively high cancer risk for ILCR > 10^{-4} [36].

3. Results and Discussion

3.1. Impact of Lockdown Measures on ΣPAHs

During the BL, DL, and AL stages, there was a strong correlation between the total PAH concentration (ΣPAHs) in $PM_{2.5}$ at the PD and DS sites. The correlation coefficients are 0.89, 0.85, and 0.87, respectively. At the same time, a strong correlation (r > 0.90) was found between the $PM_{2.5}$ concentrations at the two monitoring sites, indicating that $PM_{2.5}$ in Shanghai has strong regional pollution characteristics. The sources of PAHs at the two sites are similar or the influencing factors could be similar. Meanwhile, noticeable differences in the concentration of ΣPAHs between the two stations were observed. The concentration of ΣPAHs at the DS station was significantly higher than that at the PD station (Table 1), which is statistically significant ($p < 0.05$), indicating that the anthropogenic pollution at the DS station was significantly higher than that at the PD station. The concentration of PAHs in this study is lower than what has been observed in Shanghai from 2014 to 2017 [37,38], which is consistent with the fact that the air quality in Shanghai is improving in recent years.

Table 1. PAHs concentrations at Pudong and Qingpu sites.

Periods		bL	BL	dL	DL	aL	AL
PD	Conc. (ng/m^3)	5.63 ± 3.96	6.24 ± 4.06	4.42 ± 1.40	3.38 ± 2.43	1.85 ± 1.05	1.46 ± 0.95
	P/P variation [a]			0.79	0.54	0.33	0.23
	Y/Y variation [b]	1.11		0.76		0.79	
DS	Conc. (ng/m^3)	8.82 ± 7.27	8.89 ± 6.25	6.58 ± 2.38	4.64 ± 2.58	2.76 ± 2.16	2.70 ± 2.04
	P/P variation			0.75	0.52	0.31	0.30
	Y/Y variation	1.01		0.70		0.97	

[a] P/P variation means the relative concentration in the lockdown period and the recovery period to what was measured in the before lockdown period, respectively. [b] Y/Y variation is the ratio of concentration measured in each period during 2020 to the same period in 2019.

The concentration of PAHs in $PM_{2.5}$ had obvious temporal changes during the three stages in 2019 and 2020, namely, BL > DL > AL (Table 1), which is mainly due to the change of the atmospheric boundary layer height caused by temperature change [39]. It should be noted that the three observation periods (BL, DL, and AL periods) are the transition periods from winter to summer in Shanghai. With the increase in temperature (from an average of about 8 °C before the epidemic to an average of about 21 °C during the recovery period), the height of the atmospheric boundary layer increases, and the concentration of PAHs decreases. The above temporal changes also indicate that it is not enough to only look at the changes of pollutant concentration in different stages of the year when investigating the impact of epidemic control measures on air quality, and it is also necessary to compare with the same period without the epidemic, such as 2019.

The average concentration of total PAHs (∑PAHs) was measured to be 3.38 ng m^{-3} during the DL period at the PD site, compared with 4.42 ng m^{-3} measured during dL in 2019, a decrease of 24% was observed (Table 1). Within the same year, the ∑PAHs during the dL period were found to be 21% lower than the bL period in 2019, while they were found to decrease by 46% from BL to DL in 2020. The decrease in the concentration of Σ PAHs in the 2020 DL phase was found to be significantly greater than that in the 2019 dL phase. The level of ∑PAHs was generally higher at the DS site compared to the PD site. The temporal variation of the concentration of ΣPAHs at the DS station showed consistency with the PD station. The measured ∑PAHs at the DS site were found to undergo a reduction of 29% compared to the same period in 2019. According to the results of an independent *t*-test analysis, the difference in ∑PAHs in 2019 and 2020 was only significant between the dL and DL period ($p < 0.05$) at both sites. Thus, conclusions can be made that the COVID-19 lockdown measures led to a significant reduction in the total concentration of particulate PAHs in Shanghai.

Traffic was the emission source mostly affected by the COVID-19 lockdown in the year 2020, which may be responsible for the significant decline in ∑PAH observed during DL at both sites. According to the information from the Shanghai Municipal Bureau of Statistics, the number of passengers in railways, harbors, highways, and airports from February to May 2020 was found to have significantly decreased by 92%, 83%, 71%, and 59% compared to the same period in 2019. At the same time, some industrial activities are relatively less affected by the epidemic control strategies. From January to March 2020, the decline of the total industrial output value of electronic power, heat, gas production and supply, chemical raw materials, and chemical products manufacturing industries was found to be less than 10%, and the communications, electronic equipment manufacturing, and metal smelting and processing industries were only slightly affected [40]. As a result, the configuration of air pollution emission sources in Shanghai changed significantly during the lockdown period. The impact of such emission variation on the particulate PAHs composition will be discussed in the following section.

3.2. Lockdown Impact on the Composition of PAHs

3.2.1. Variation of PAH Monomer Distribution

BbkF was found to be the most abundant PAH monomer during the whole sampling period, while Phe, Flu, Pyr, Chr, BeP, IcdP, and BghiP were found to be other monomeric PAH compounds with relatively high contents in $PM_{2.5}$ (Figure 2), exceeding 75% of ΣPAHs. Such a finding is consistent with the reported PAH composition in Shanghai and the Yangtze River Delta ambient particles [37,38]. The maximum concentration of strongly carcinogenic monomer BaP was measured to be 1.2 ng m^{-3}, which is lower than the standard limit of 2.5 ng m^{-3} of the daily average value listed in the Ambient Air Quality Standard (GB3095-2012). Except for QP and Cor, the concentrations of different PAH monomers were found to be significantly correlated with the concentration of ΣPAHs ($r > 0.85$, $p < 0.01$), indicating that the composition of PAHs in Shanghai was relatively stable during the observation period.

As indicated in Figure 2, although the relative content of QP and Cor changed significantly in the DL and AL stages, the relative distributions of PAH monomers (percentage of PAHs monomer concentration in ΣPAHs concentration) during the three observation periods in 2019 (bL, dL, and aL) and 2020 (BL, DL, and AL) are very similar, which is consistent with the correlation between PAHs monomer and ΣPAHs. QP has been reported to be an indicator of waste incineration [41]. The relative content of QP during the DL phase at the PD site was measured to be 2 times higher than what was measured during the dL phase, and the relative content of QP during the AL phase was measured to be 1.4 times higher than what was measured during the aL phase. Such an increase in the relative content of QP during the DL stage indicated an enhancement in the potential impact of unorganized sources such as waste incineration. However, future evidence should be provided in order to confirm this phenomenon. The relative content of Cor had similar variations at both sites. Taking the PD site as an example, the relative content of Cor during the DL phase was measured to be 39% of that during the dL phase, and 65% when comparing the AL to the aL phase. It should be noted that Cor can be used as an indicator of vehicle exhaust [42].

In combination with strict traffic control measures during the pandemic lockdown, the sharp decline in the concentration of Cor indicates a significant decrease from motor vehicle emissions, which also reflects that other PAH monomers may be a poor indicator for traffic emissions. The highly consistent distribution of PAH monomers during different periods in 2020 and 2019 illustrates that lockdown measures had a negligible impact on the relative composition of particulate PAHs in Shanghai.

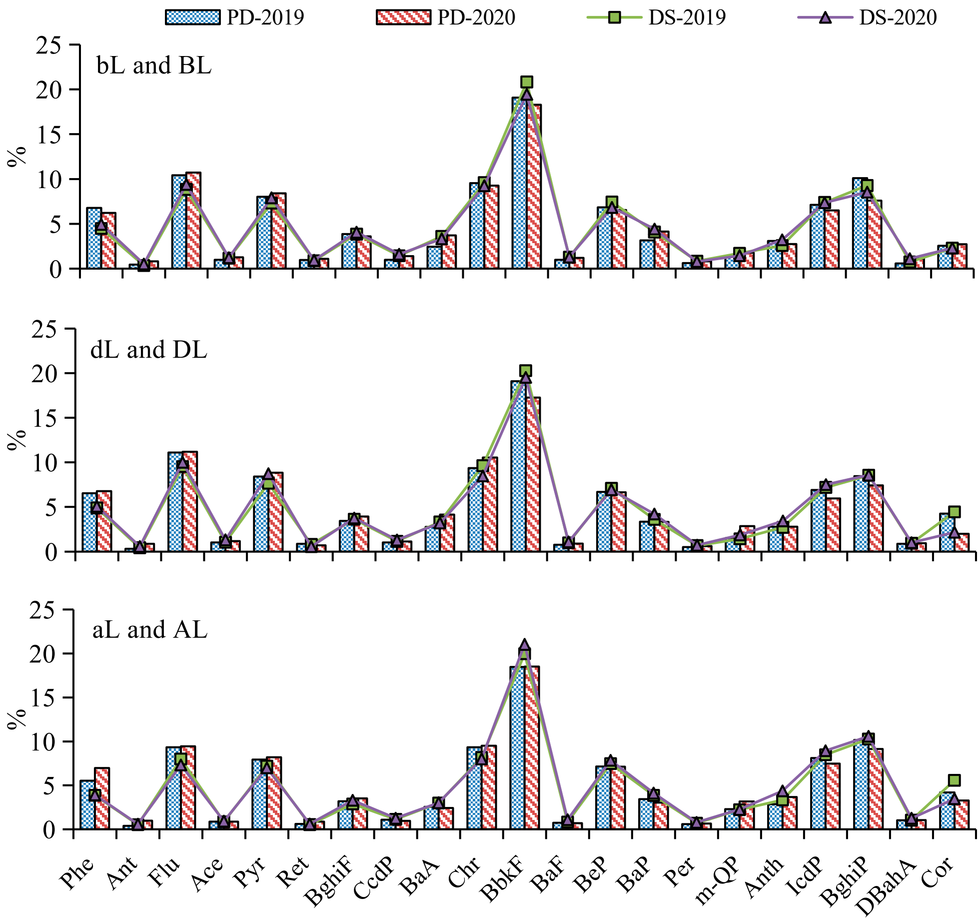

Figure 2. Relative concentrations of PAHs monomers during three stages at PD and DS.

By comparing the distribution of PAH monomers during the three stages in the same year, the major difference in PAH composition at different stages was mainly manifested in the relative content of low molecular-weight PAHs (LMW PAHs, with molecular weight less than 228 Da.). During the AL period, the relative content of LMW PAHs was found to be lower, while the relative content of high molecular weight PAHs (HMW PAHs, with a molecular weight greater than 252 Da.) was found to be significantly higher compared to the BL and DL stages. Taking DS as an example, the LMW/HMW ratios during BL, DL, and AL periods were 0.80, 0.76, and 0.56, respectively. This trend may be attributed to the varied gas-particle partitioning of semi-volatile PAHs under the impact of increasing temperature [29,43]. LMW PAHs are more volatile, and tend to stay in the gas phase when the temperature rises. Therefore, the increase in the relative particulate content of HMW PAHs during the recovery period after the pandemic lockdown may be attributed to the enhanced ambient temperature, instead of the variation of the emission source, such as the recovery of vehicle exhaust.

3.2.2. Variation of the Aromatic Ring Distribution

Figure 3 indicates the relative concentration of PAH monomers with different benzene rings in $PM_{2.5}$ during different observation periods, among which PAHs with four and five rings are the dominant species (accounting for 30–40% of total particulate PAHs measured) while three-ring and six-ring PAHs constituted a less significant fraction (10–20% of the total particulate PAHs measured). The overall distributions of PAHs look similar at the PD and the DS site, while four-ring PAHs were found to be less abundant (around 10%) and five-ring PAHs were found to be more abundant (around 10%) at the DS site compared to PD, illustrating the impact of local sources on the composition of PAHs in Shanghai. This is consistent with the significant difference observed in the PAH concentrations between the two sites. As indicated in Figure 3, the distribution of the ring number of PAHs exhibits annual consistency comparing 2019 to 2020. For example, the relative abundances of PAHs with three to four rings were observed to follow DL > BL > AL at both the PD site and the DS site. However, the differences observed for the relative abundance of three- to four-ring PAHs across the three observation periods were not statistically significant, indicating that the slight enhancement of PAHs with three to four rings during the DL period may not directly benefit from the traffic and industrial lockdown due to the pandemic.

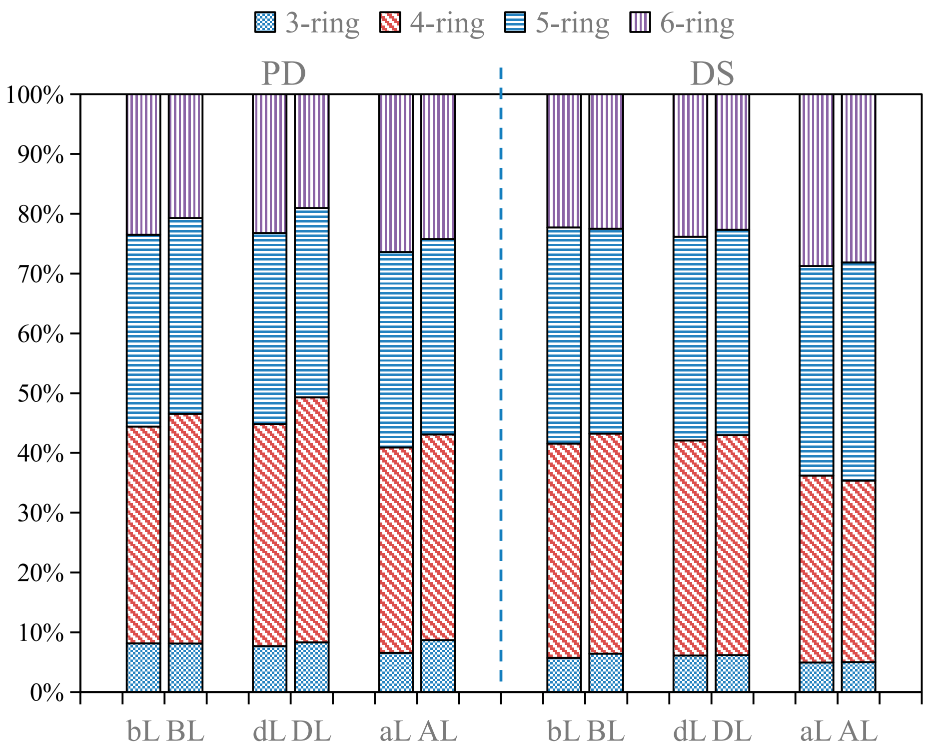

Figure 3. Relative contribution of PAHs with different number of benzene rings in each period from 2019 to 2020.

As discussed above, the abrupt change in anthropogenic emission, especially traffic emission, during the pandemic lockdown didn't directly result in significant variations in the PAH composition, which is consistent for different zones with different pollution levels in Shanghai (i.e., PD vs. DS). The result of the current study suggests that traffic might not be the major source of PAHs in Shanghai nowadays. Alternatively, PAHs in $PM_{2.5}$ from different emission sources in Shanghai might have similar compositions.

3.3. Impact of Lockdown on PAHs Sources

Previous works put forward that specific diagnostic ratios between PAH monomers can be used to indicate the source of PAHs in the ambient air [44,45]. For example, PAHs emitted from the traffic source were normally identified with the Flu/(Flu + Pyr) < 0.5, while Flu/(Flu + Pyr) > 0.5 and IcdP/(IcdP + BghiP) > 0.5 are indicators for PAHs emitted from coal/biomass burning [46]. Figure 4 illustrates the distribution of Flu/(Flu + Pyr) and IcdP/(IcdP + BghiP) at the PD and DS sites. The distribution of the Flu/(Flu + Pyr) ratio indicates that the major source of PAHs during the three different observation periods is coal/biomass burning for both monitoring sites. However, the distribution of the IcdP/(IcdP + BghiP) ratio indicated that traffic emission might also be the dominant emission source during the three observation periods at both sites. Positive matrix factorization (PMF) analysis has been widely applied to identify the source of PAHs in $PM_{2.5}$ [47]. In a previous study, coal burning (30.5%) and gasoline engine emission (29.0%) were identified by source apportionment as the two major sources of PAHs in $PM_{2.5}$ samples collected in Shanghai [20]. More recently, the major sources for particulate PAHs in Shanghai were identified to be vehicle emissions and coal or biomass combustion using PMF [19]. Though the physicochemical characteristics of the above-mentioned PAH monomers are similar, certain differences still exist in the volatility and thus the gas-particle partitioning behaviors among individual PAH compounds. The contradictory indication from the PAH diagnostic ratios above suggests that caution should be taken while using those ratios for PAH source identification in future studies.

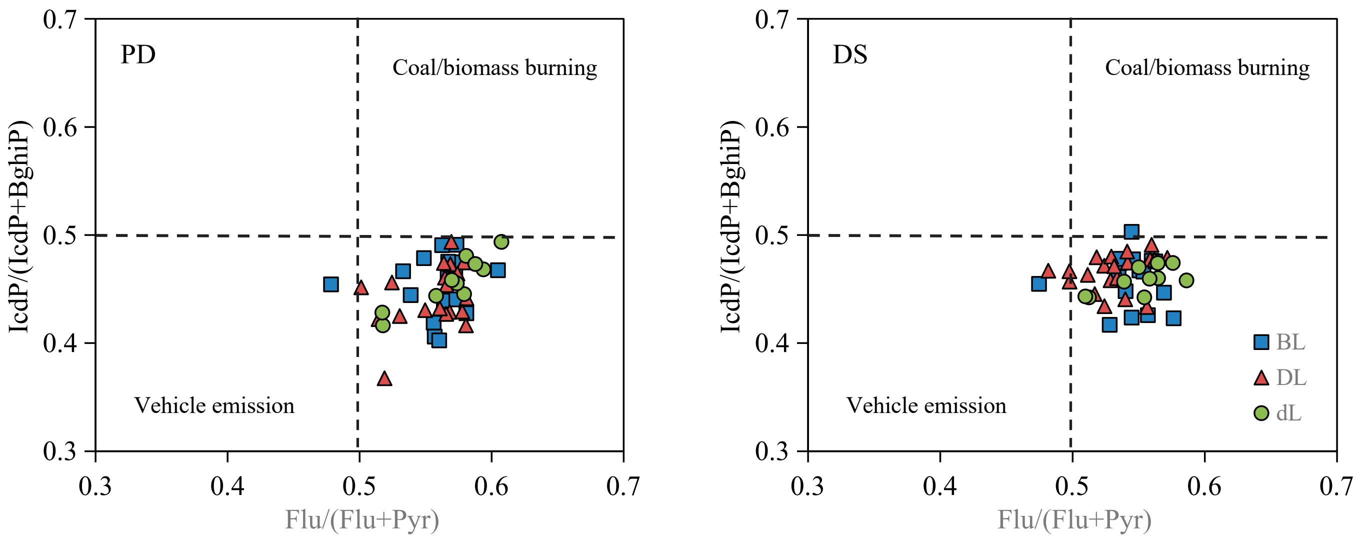

Figure 4. Source identification plots for Flu/(Flu + Pyr) and IcdP/(IcdP + BghiP).

As illustrated in Figure 4, the characteristics of PAHs in the DL period exhibited no significant difference from other periods. The sudden drop in traffic activities during the lockdown period in Shanghai did not impact the characteristics of local PAH composition significantly, which reflected that most of the PAH monomers may not be representative enough to be used for traffic emission indicators in this region except for coronene. As a result, except for some typical scenarios, it is currently challenging to judge the source of PAHs merely based on their chemical compositions, which potentially share many characteristics in common with different emission sources in urban regions.

3.4. Health Risk Evaluation of PAHs

PAHs and their derivatives in the atmosphere, especially nitrated and oxygenated PAHs, are known to be carcinogenic and mutagenic, leading to significant adverse health outcomes upon exposure [48–52]. Given their lipophilic molecular specialty, PAHs can directly penetrate the phospholipid bilayer of the cell membrane [53]. Acting as ligands for aryl hydrocarbon receptor (AhR), PAHs can also activate AhR and upregulate cytochrome P450 (CYP) metabolizing enzymes to initiate the redox-cycling metabolism and produce reactive oxygen species (ROS) [54]. Both the primary and secondary PAH content in urban ambient particles were found to be associated with the level of inflammatory cytokines (e.g., IL-2, IL-6, and IL-8) [51,55]. A previous study observed that the expression of cellular heme oxygenase-1 (HO-1), a sensitive marker for oxidative stress, is directly correlated with the high PAH content of ultra-fine particles [56].

As indicated in Table 2, the BaP_{eq} during the 2020 lockdown period was found to decrease by 23% and 24% compared to the dL period in 2019 for the PD and DS site, respectively. However, the pandemic lockdown measurement did not exert significant impacts on the composition of PAHs in $PM_{2.5}$ at both sites. PAHs with the most significant BaP_{eq} values were consistently found to be BaP, BbkF, DBahA, IcdP, and BaA across all three observation periods for both sites, among which BaP contributed more than 45% of the estimated BaP_{eq}.

Table 2. BaP_{eq} and ILCR in different periods in Shanghai.

Periods		bL	BL	dL	DL	aL	AL
PD	BaP_{eq} (ng/m^3)	0.38	0.52	0.32	0.25	0.14	0.11
	ILCR (10^{-5})	3.33	4.53	2.82	2.16	1.24	0.92
DS	BaP_{eq} (ng/m^3)	0.71	0.77	0.52	0.40	0.23	0.24
	ILCR (10^{-5})	6.19	6.74	4.53	3.44	2.01	2.11

During the COVID-19 lockdown period, the estimated ILCR was found to be within the range of 3.8×10^{-6}~9.5×10^{-5} upon inhaling PAHs in Shanghai, indicating a potential cancer risk. Due to the COVID-19 lockdown measurements, the ILCR at the PD and the DS site was estimated to be 2.16×10^{-5}~3.44×10^{-5}, respectively, with a decrease of around 25%. Our observation indicated that even with the first level public health alert, exposure to PAHs can still potentially cause cancer risks. More strategies should be designed in order to control PAH-related pollution and the corresponding health risks in the future.

4. Conclusions

PAHs are major hazardous semi-volatile organic species in the urban atmosphere, with both carcinogenic and mutagenic health effects on the residential population. In this study, $PM_{2.5}$ samples were collected during three stages in 2019 (bL, dL, and aL) and 2020 (BL, DL, and AL) in order to analyze the potential impacts of the COVID-19 lockdown on the content of particulate PAHs. Overall, 21 different types of PAHs were characterized using the GC-MS method. Major conclusions of the current work include: The abundance of PAHs in $PM_{2.5}$ decreased significantly during the pandemic lockdown while the relative abundance of different PAH monomers remained similar during three observation period (BL, DL and AL) in 2020 compared to the same periods in 2019. The relative abundance of low molecular weight PAHs decreased significantly during the AL period compared to the previous observation periods (i.e., BL and DL), which might be resulted from the warming temperature effect on the gas-particle partitioning of semi-volatile PAHs. Based on the results from specific diagnostic ratios between PAH monomers, both vehicular and coal/biomass burning could be potential sources of PAHs during the observation periods in Shanghai. The similarity of the composition of PAHs in terms of different areas and periods in Shanghai may bring significant uncertainties to the source identification of PAHs. During the COVID-19 lockdown, the BaP equivalent toxicity was observed to decrease by 24% compared to the period before the lockdown. Despite this, exposure to such PAH levels can still potentially lead to significant cancer risk in the exposure population. As a result, more specific source identification methods for PAHs should be investigated and more stringent strategies for the mitigation of PAHs in urban areas are warranted in future investigations.

Author Contributions: Conceptualization, J.F. and S.W.; methodology, J.F.; formal analysis, F.F., Y.F., M.H. and J.C.; investigation, J.F. and S.W.; resources, J.F. and Q.F.; data curation, J.F. and S.W.; writing—original draft preparation, J.F.; writing—review and editing, J.F., Y.S. and S.W.; visualization, F.F. and Y.F.; supervision, J.F. and S.W.; project administration, J.F. and Q.F.; funding acquisition, J.F. All authors have read and agreed to the published version of the manuscript.

Funding: This research was financially supported by the National Natural Science Foundation of China (Grant No: 41877373).

Institutional Review Board Statement: Not applicable.

Informed Consent Statement: Not applicable.

Data Availability Statement: The data that support the findings of this study are available from the corresponding author, upon reasonable request.

Conflicts of Interest: The authors declare no conflict of interest.

References

1. Abdel-Shafy, H.I.; Mansour, M.S.M. A review on polycyclic aromatic hydrocarbons: Source, environmental impact, effect on human health and remediation. *Egypt. J. Pet.* **2016**, *25*, 107–123. [CrossRef]
2. Dat, N.-D.; Chang, M.B. Review on characteristics of PAHs in atmosphere, anthropogenic sources and control technologies. *Sci. Total. Environ.* **2017**, *609*, 682–693. [CrossRef] [PubMed]
3. Liu, S.; Tao, S.; Liu, W.; Liu, Y.; Dou, H.; Zhao, J.; Wang, L.; Wang, J.; Tian, Z.; Gao, Y. Atmospheric Polycyclic Aromatic Hydrocarbons in North China: A Winter-Time Study. *Environ. Sci. Technol.* **2007**, *41*, 8256–8261. [CrossRef] [PubMed]
4. Byambaa, B.; Yang, L.; Matsuki, A.; Nagato, E.G.; Gankhuyag, K.; Chuluunpurev, B.; Banzragch, L.; Chonokhuu, S.; Tang, N.; Hayakawa, K. Sources and Characteristics of Polycyclic Aromatic Hydrocarbons in Ambient Total Suspended Particles in Ulaanbaatar City, Mongolia. *Int. J. Environ. Res. Public Health* **2019**, *16*, 442. [CrossRef] [PubMed]
5. Elzein, A.; Dunmore, R.E.; Ward, M.W.; Hamilton, J.F.; Lewis, A.C. Variability of polycyclic aromatic hydrocarbons and their oxidative derivatives in wintertime Beijing, China. *Atmos. Chem. Phys.* **2019**, *19*, 8741–8758. [CrossRef]
6. Ihunwo, O.C.; Shahabinia, A.R.; Udo, K.S.; Bonnail, E.; Onyema, M.O.; Orji, A.N.D.; Mmom, P.C. Distribution of polycyclic aromatic hydrocarbons in Woji Creek, in the Niger Delta. *Environ. Res. Commun.* **2019**, *1*, 125001. [CrossRef]
7. Zhang, Y.J.; Lin, Y.; Cai, J.; Liu, Y.; Hong, L.N.; Qin, M.M.; Zhao, Y.F.; Ma, J.; Wang, X.S.; Zhu, T.; et al. Atmospheric PAHs in North China: Spatial distribution and sources. *Sci. Total Environ.* **2016**, *565*, 994–1000. [CrossRef] [PubMed]
8. Sushkova, S.; Minkina, T.; Deryabkina, I.; Rajput, V.; Antonenko, E.; Nazarenko, O.; Yadav, B.K.; Hakki, E.; Mohan, D. Environmental pollution of soil with PAHs in energy producing plants zone. *Sci. Total. Environ.* **2019**, *655*, 232–241. [CrossRef]
9. Premnath, N.; Mohanrasu, K.; Rao, R.G.R.; Dinesh, G.; Prakash, G.S.; Ananthi, V.; Ponnuchamy, K.; Muthusamy, G.; Arun, A. A crucial review on polycyclic aromatic Hydrocarbons-Environmental occurrence and strategies for microbial degradation. *Chemosphere* **2021**, *280*, 130608. [CrossRef]
10. Foan, L.; Leblond, S.; Thöni, L.; Raynaud, C.; Santamaria, J.M.; Sebilo, M.; Simon, V. Spatial distribution of PAH concentrations and stable isotope signatures (δ13C, δ15N) in mosses from three European areas–Characterization by multivariate analysis. *Environ. Pollut.* **2014**, *184*, 113–122. [CrossRef]
11. Poster, D.L.; Schantz, M.M.; Sander, L.C.; Wise, S.A. Analysis of polycyclic aromatic hydrocarbons (PAHs) in environmental samples: A critical review of gas chromatographic (GC) methods. *Anal. Bioanal. Chem.* **2006**, *386*, 859–881. [CrossRef] [PubMed]
12. Mesquita, S.R.; van Drooge, B.L.; Barata, C.; Vieira, N.; Guimaraes, L.; Piña, B. Toxicity of atmospheric particle-bound PAHs: An environmental perspective. *Environ. Sci. Pollut. Res.* **2014**, *21*, 11623–11633. [CrossRef] [PubMed]
13. Lin, Y.; Ma, Y.; Qiu, X.; Li, R.; Fang, Y.; Wang, J.; Zhu, Y.; Hu, D. Sources, transformation, and health implications of PAHs and their nitrated, hydroxylated, and oxygenated derivatives in $PM_{2.5}$ in Beijing. *J. Geophys. Res. Atmos.* **2015**, *120*, 7219–7228. [CrossRef]
14. He, J.; Balasubramanian, R. Determination of Atmospheric Polycyclic Aromatic Hydrocarbons Using Accelerated Solvent Extraction. *Anal. Lett.* **2009**, *42*, 1603–1619. [CrossRef]
15. Mahato, S.; Pal, S.; Ghosh, K.G. Effect of lockdown amid COVID-19 pandemic on air quality of the megacity Delhi, India. *Sci. Total. Environ.* **2020**, *730*, 139086. [CrossRef] [PubMed]
16. Collivignarelli, M.C.; Abbà, A.; Bertanza, G.; Pedrazzani, R.; Ricciardi, P.; Miino, M.C. Lockdown for CoViD-2019 in Milan: What are the effects on air quality? *Sci. Total Environ.* **2020**, *732*, 139280. [CrossRef] [PubMed]
17. Okuda, T.; Naoi, D.; Tenmoku, M.; Tanaka, S.; He, K.; Ma, Y.; Yang, F.; Lei, Y.; Jia, Y.; Zhang, D. Polycyclic aromatic hydrocarbons (PAHs) in the aerosol in Beijing, China, measured by aminopropylsilane chemically-bonded stationary-phase column chromatography and HPLC/fluorescence detection. *Chemosphere* **2006**, *65*, 427–435. [CrossRef]
18. Cao, J.-J.; Zhu, C.-S.; Tie, X.-X.; Geng, F.-H.; Xu, H.-M.; Ho, S.S.H.; Wang, G.-H.; Han, Y.-M.; Ho, K.-F. Characteristics and sources of carbonaceous aerosols from Shanghai, China. *Atmos. Chem. Phys.* **2013**, *13*, 803–817. [CrossRef]
19. Wei, X.-Y.; Liu, M.; Yang, J.; Du, W.-N.; Sun, X.; Huang, Y.-P.; Zhang, X.; Khalil, S.K.; Luo, D.-M.; Zhou, Y.-D. Characterization of PM2.5-bound PAHs and carbonaceous aerosols during three-month severe haze episode in Shanghai, China: Chemical composition, source apportionment and long-range transportation. *Atmos. Environ.* **2019**, *203*, 1–9. [CrossRef]
20. Wang, F.; Lin, T.; Feng, J.; Fu, H.; Guo, Z. Source apportionment of polycyclic aromatic hydrocarbons in PM2.5 using positive matrix factorization modeling in Shanghai, China. *Environ. Sci. Process. Impacts* **2015**, *17*, 197–205. [CrossRef]
21. Venter, Z.S.; Aunan, K.; Chowdhury, S.; Lelieveld, J. COVID-19 lockdowns cause global air pollution declines. *Proc. Natl. Acad. Sci. USA* **2020**, *117*, 18984–18990. [CrossRef] [PubMed]

22. Lian, X.; Huang, J.; Huang, R.; Liu, C.; Wang, L.; Zhang, T. Impact of city lockdown on the air quality of COVID-19-hit of Wuhan city. *Sci. Total. Environ.* **2020**, *742*, 140556. [CrossRef]
23. He, G.; Pan, Y.; Tanaka, T. The short-term impacts of COVID-19 lockdown on urban air pollution in China. *Nat. Sustain.* **2020**, *3*, 1005–1011. [CrossRef]
24. Chauhan, A.; Singh, R.P. Decline in PM2.5 concentrations over major cities around the world associated with COVID-19. *Environ. Res.* **2020**, *187*, 109634. [CrossRef]
25. Fuwape, I.A.; Okpalaonwuka, C.T.; Ogunjo, S.T. Impact of COVID-19 pandemic lockdown on distribution of inorganic pollutants in selected cities of Nigeria. *Air Qual. Atmos. Health* **2021**, *14*, 149–155. [CrossRef]
26. Kerimray, A.; Baimatova, N.; Ibragimova, O.; Bukenov, B.; Kenessov, B.; Plotitsyn, P.; Karaca, F. Assessing air quality changes in large cities during COVID-19 lockdowns: The impacts of traffic-free urban conditions in Almaty, Kazakhstan. *Sci. Total. Environ.* **2020**, *730*, 139179. [CrossRef]
27. Balmer, J.E.; Hung, H.; Yu, Y.; Letcher, R.J.; Muir, D.C. Sources and environmental fate of pyrogenic polycyclic aromatic hydrocarbons (PAHs) in the Arctic. *Emerg. Contam.* **2019**, *5*, 128–142. [CrossRef]
28. Howsam, M.; Jones, K.C. Sources of PAHs in the environment. In *PAHs and Related Compounds*; Springer: Berlin/Heidelberg, Germany, 1998; pp. 137–174. [CrossRef]
29. Feng, J.; Hu, M.; Chan, C.K.; Lau, P.S.; Fang, M.; He, L.; Tang, X. A comparative study of the organic matter in PM2.5 from three Chinese megacities in three different climatic zones. *Atmos. Environ.* **2006**, *40*, 3983–3994. [CrossRef]
30. Nisbet, I.C.T.; Lagoy, P.K. Toxic equivalency factors (TEFs) for polycyclic aromatic hydrocarbons (PAHs). *Regul. Toxicol. Pharmacol.* **1992**, *16*, 290–300. [CrossRef] [PubMed]
31. Samburova, V.; Connolly, J.; Gyawali, M.; Yatavelli, R.L.; Watts, A.C.; Chakrabarty, R.K.; Zielinska, B.; Moosmüller, H.; Khlystov, A. Polycyclic aromatic hydrocarbons in biomass-burning emissions and their contribution to light absorption and aerosol toxicity. *Sci. Total Environ.* **2016**, *568*, 391–401. [CrossRef]
32. Chang, K.-F.; Fang, G.-C.; Chen, J.-C.; Wu, Y.-S. Atmospheric polycyclic aromatic hydrocarbons (PAHs) in Asia: A review from 1999 to 2004. *Environ. Pollut.* **2006**, *142*, 388–396. [CrossRef] [PubMed]
33. Lee, B.-K.; Dong, T.T. Effects of road characteristics on distribution and toxicity of polycyclic aromatic hydrocarbons in urban road dust of Ulsan, Korea. *J. Hazard. Mater.* **2010**, *175*, 540–550. [CrossRef]
34. Halek, F.; Nabi, G.; Kavousi, A. Polycyclic aromatic hydrocarbons study and toxic equivalency factor (TEFs) in Tehran, IRAN. *Environ. Monit. Assess.* **2008**, *143*, 303–311. [CrossRef]
35. Cincinelli, A.; Del Bubba, M.; Martellini, T.; Gambaro, A.; Lepri, L. Gas-particle concentration and distribution of n-alkanes and polycyclic aromatic hydrocarbons in the atmosphere of Prato (Italy). *Chemosphere* **2007**, *68*, 472–478. [CrossRef]
36. Xia, Z.; Duan, X.; Tao, S.; Qiu, W.; Liu, D.; Wang, Y.; Wei, S.; Wang, B.; Jiang, Q.; Lu, B.; et al. Pollution level, inhalation exposure and lung cancer risk of ambient atmospheric polycyclic aromatic hydrocarbons (PAHs) in Taiyuan, China. *Environ. Pollut.* **2013**, *173*, 150–156. [CrossRef] [PubMed]
37. Liu, Y.; Yu, Y.; Liu, M.; Lu, M.; Ge, R.; Li, S.; Liu, X.; Dong, W.; Qadeer, A. Characterization and source identification of PM2.5-bound polycyclic aromatic hydrocarbons (PAHs) in different seasons from Shanghai, China. *Sci. Total Environ.* **2018**, *644*, 725–735. [CrossRef] [PubMed]
38. Jia, J.; Deng, L.; Bi, C.; Jin, X.; Zeng, Y.; Chen, Z. Seasonal variations, gas-PM2.5 partitioning and long-distance input of PM2.5-bound and gas-phase polycyclic aromatic hydrocarbons in Shanghai, China. *Atmos. Environ.* **2021**, *252*, 118335. [CrossRef]
39. Kubo, T.; Bai, W.; Nagae, M.; Takao, Y. Seasonal Fluctuation of Polycyclic Aromatic Hydrocarbons and Aerosol Genotoxicity in Long-Range Transported Air Mass Observed at the Western End of Japan. *Int. J. Environ. Res. Public Health* **2020**, *17*, 1210. [CrossRef]
40. Fan, F.; Feng, Y.; Feng, J.; Hu, M.; Ye, J.; Tian, M.; Fu, Q. Molecular Tracer Characterization during COVID-19 Pandemic in Shanghai: Changes in the Aerosol Aqueous Environment and Implications for Secondary Organic Aerosol Formation. *ACS Earth Space Chem.* **2022**, *6*, 2812–2825. [CrossRef]
41. Hawley-Fedder, R.; Parsons, M.; Karasek, F. Products obtained during combustion of polymers under simulated incinerator conditions: II. Polystyrene. *J. Chromatogr. A* **1984**, *315*, 201–210. [CrossRef]
42. Nielsen, T. Traffic contribution of polycyclic aromatic hydrocarbons in the center of a large city. *Atmos. Environ.* **1996**, *30*, 3481–3490. [CrossRef]
43. Wang, C.; Wang, X.; Gong, P.; Yao, T. Polycyclic aromatic hydrocarbons in surface soil across the Tibetan Plateau: Spatial distribution, source and air–soil exchange. *Environ. Pollut.* **2014**, *184*, 138–144. [CrossRef] [PubMed]
44. Liu, Y.; Yan, C.; Ding, X.; Wang, X.; Fu, Q.; Zhao, Q.; Zhang, Y.; Duan, Y.; Qiu, X.; Zheng, M. Sources and spatial distribution of particulate polycyclic aromatic hydrocarbons in Shanghai, China. *Sci. Total. Environ.* **2017**, *584–585*, 307–317. [CrossRef] [PubMed]
45. Tobiszewski, M.; Namieśnik, J. PAH diagnostic ratios for the identification of pollution emission sources. *Environ. Pollut.* **2012**, *162*, 110–119. [CrossRef] [PubMed]
46. Yunker, M.B.; Macdonald, R.W.; Vingarzan, R.; Mitchell, R.H.; Goyette, D.; Sylvestre, S. PAHs in the Fraser River basin: A critical appraisal of PAH ratios as indicators of PAH source and composition. *Org. Geochem.* **2002**, *33*, 489–515. [CrossRef]
47. Sofowote, U.M.; McCarry, B.E.; Marvin, C.H. Source Apportionment of PAH in Hamilton Harbour Suspended Sediments: Comparison of Two Factor Analysis Methods. *Environ. Sci. Technol.* **2008**, *42*, 6007–6014. [CrossRef]

48. Khan, S.; Cao, Q. Human health risk due to consumption of vegetables contaminated with carcinogenic polycyclic aromatic hydrocarbons. *J. Soils Sediments* **2012**, *12*, 178–184. [CrossRef]
49. Omar, N.Y.M.; Mon, T.C.; Rahman, N.A.; Bin Abas, M.R. Distributions and health risks of polycyclic aromatic hydrocarbons (PAHs) in atmospheric aerosols of Kuala Lumpur, Malaysia. *Sci. Total Environ.* **2006**, *369*, 76–81. [CrossRef]
50. Pashin, Y.V.; Bakhitova, L. Mutagenic and carcinogenic properties of polycyclic aromatic hydrocarbons. *Environ. Health Perspect.* **1979**, *30*, 185–189. [CrossRef]
51. Shiraiwa, M.; Selzle, K.; Pöschl, U. Hazardous components and health effects of atmospheric aerosol particles: Reactive oxygen species, soot, polycyclic aromatic compounds and allergenic proteins. *Free Radic. Res.* **2012**, *46*, 927–939. [CrossRef]
52. Durant, J.L.; Busby, W.F., Jr.; Lafleur, A.L.; Penman, B.W.; Crespi, C.L. Human cell mutagenicity of oxygenated, nitrated and unsubstituted polycyclic aromatic hydrocarbons associated with urban aerosols. *Mutat. Res. Genet. Toxicol.* **1996**, *371*, 123–157. [CrossRef]
53. Pardo, M.; Qiu, X.; Zimmermann, R.; Rudich, Y. Particulate Matter Toxicity Is Nrf2 and Mitochondria Dependent: The Roles of Metals and Polycyclic Aromatic Hydrocarbons. *Chem. Res. Toxicol.* **2020**, *33*, 1110–1120. [CrossRef] [PubMed]
54. Penning, T.M.; Burczynski, M.E.; Hung, C.-F.; McCoull, K.D.; Palackal, A.N.T.; Tsuruda, L.S. Dihydrodiol Dehydrogenases and Polycyclic Aromatic Hydrocarbon Activation: Generation of Reactive and Redox Active *o*-Quinones. *Chem. Res. Toxicol.* **1998**, *12*, 1–18. [CrossRef] [PubMed]
55. Lerner, C.A.; Sundar, I.K.; Yao, H.; Gerloff, J.; Ossip, D.J.; McIntosh, S.; Robinson, R.; Rahman, I. Vapors Produced by Electronic Cigarettes and E-Juices with Flavorings Induce Toxicity, Oxidative Stress, and Inflammatory Response in Lung Epithelial Cells and in Mouse Lung. *PLoS ONE* **2015**, *10*, e0116732. [CrossRef] [PubMed]
56. Li, N.; Sioutas, C.; Cho, A.; Schmitz, D.; Misra, C.; Sempf, J.; Wang, M.; Oberley, T.; Froines, J.; Nel, A. Ultrafine particulate pollutants induce oxidative stress and mitochondrial damage. *Environ. Health Perspect.* **2003**, *111*, 455–460. [CrossRef] [PubMed]